Electronic Supplementary Material (ESI) for Journal of Materials Chemistry B.

Polyethyleneimine-mediated assembly of DNA nanotubes for KRAS siRNA delivery in lung adenocarcinoma therapy

Jia-Hao Bai, [#a] Qing-Tao Yu, [#a] Yi-Wu Wang, [#a] Chun-Fa Chen,[b] Lian-Ju Ma,[a] Yue Yuan,[b] Yong-Jun Gan,[a] Jia-Qi Yang,[a] Shu Zhu,[a] Yu-Hang Ran,[a] Li-Lei Zhang,[a] Hang Qian,[b] Zheng-Huan Zhao [*c] and Qian Liu [*a]

[a.] *Laboratory of Pharmacy and Chemistry, and Laboratory of Tissue and Cell Biology, Lab Teaching & Management Center, Chongqing Medical University, Chongqing 400016, China. Email: qianliu330@cqmu.edu.cn*

[b.] *Institute of Respiratory Diseases, Xinqiao Hospital, Third Military Medical University, 183 Xinqiao Street, Chongqing 400037, China. E-mail: hqian@tmmu.edu.cn*

[c.] *College of Basic Medical Sciences, Chongqing Medical University. Chongqing 400016, China. Email: roddirck@cqmu.edu.cn*

Table S1 DNA strands used for constructing PNT and PNT-KRAS nanotubes.

DNA strands	**Sequence 5’ to 3’**
L	AGG CAC CAT CGT AGG TTA TTT AAT CTT GCC AGG CAC CAT CGT AGG TTA TTT AAT CTT GCC AGG CAC CAT CGT AGG TTA TTT AAT CTT GCC
L’	GTA GGT TTT TTC TTG CCA GGC ACC ATC GTA GGT TTT TTC TTG CCA GGC ACC ATC GTA GGT TTT TTC TTG CCA GGC ACC ATC
M	TAG CAA CCT GCC TGA GCG CTT TTG CGC TGT GCA AGC CTA CGA TGG ACA CG GTA ACG AC
M’	CAA GTA GTA ATT GAT GGA GTT TTG CAA GCC TAC GAT GGA CAC GGT AAC GAC
M’’	TAG CAA CCT GCC TG
S	ACC GTG TGG TTG CTA GTC GTT

(A)

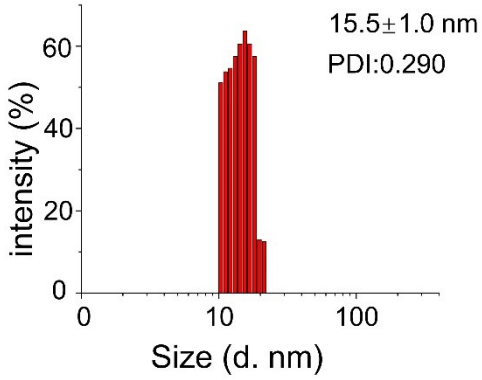

(B)

DNA nanotube	Hydrodynamic size (nm)	PDI	Zeta Potential (mV)
MNT	15.5 ± 1.0	0.290	10.5 ± 2.0
PNT	17.1 ± 2.0	0.327	3.0 ± 1.8

Fig. S1 (A) Dynamic light scattering analysis (DLS) of DNA nanotube (MNT) assembled by magnesium ions. (B) Hydrodynamic size and ζ potential comparison of PNT and MNT. Data present mean ± SD, n=3.

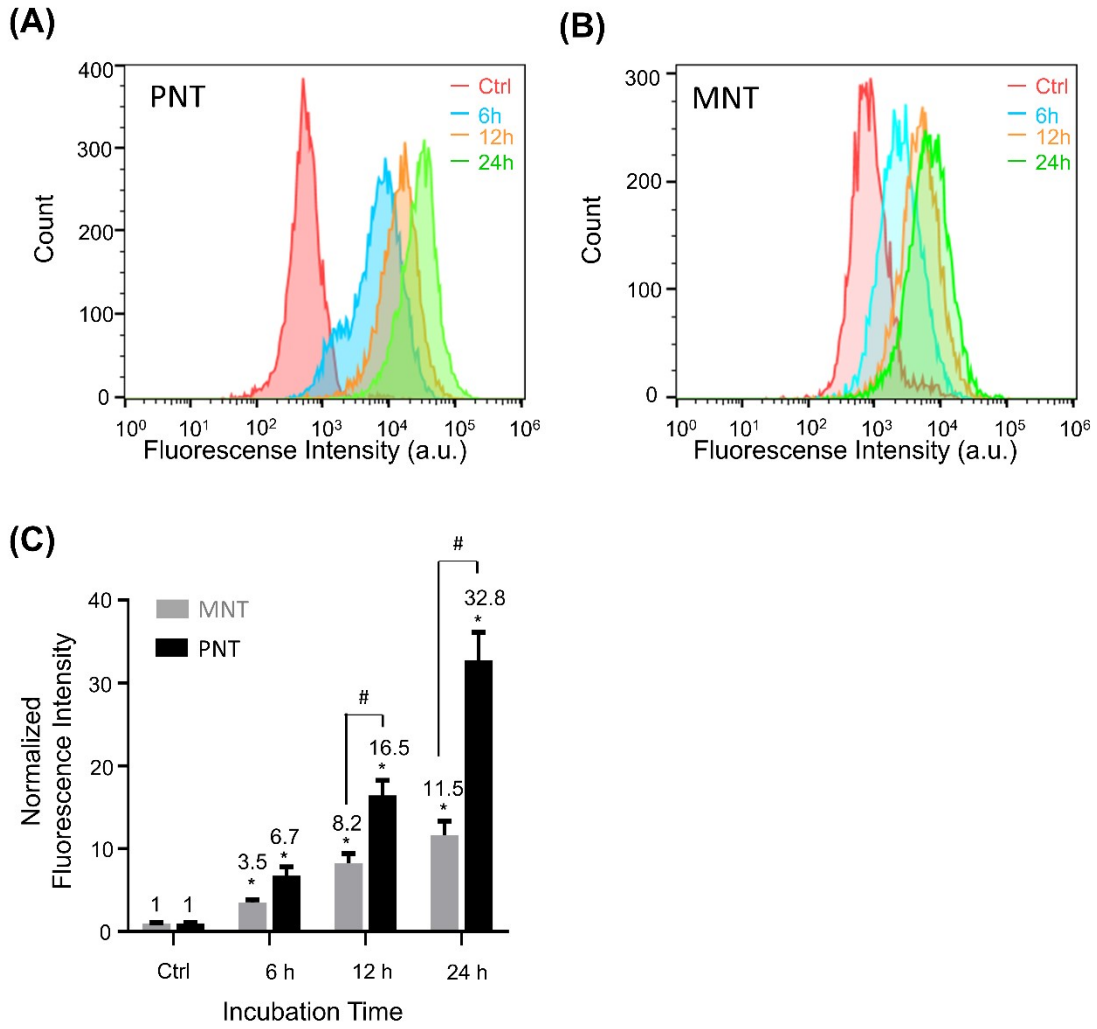

Fig. S2 Flow cytometry analysis of the internalization efficiency of PNT at various time duration. The Fluorescence intensity distribution of PNT(A) and MNT (B) was analyzed after 6 h, 12 h and 24 h of incubation. Cells incubated in pure medium served as controls. (C) A comparison of the mean fluorescence intensity between PNT and MNT was conducted at each time point. Data present as mean value ±SD (n=3). One-Way ANOVA was used for statistical analysis. * $P<0.05$, compared to the control group. # $P<0.01$, comparison between the two connected groups.

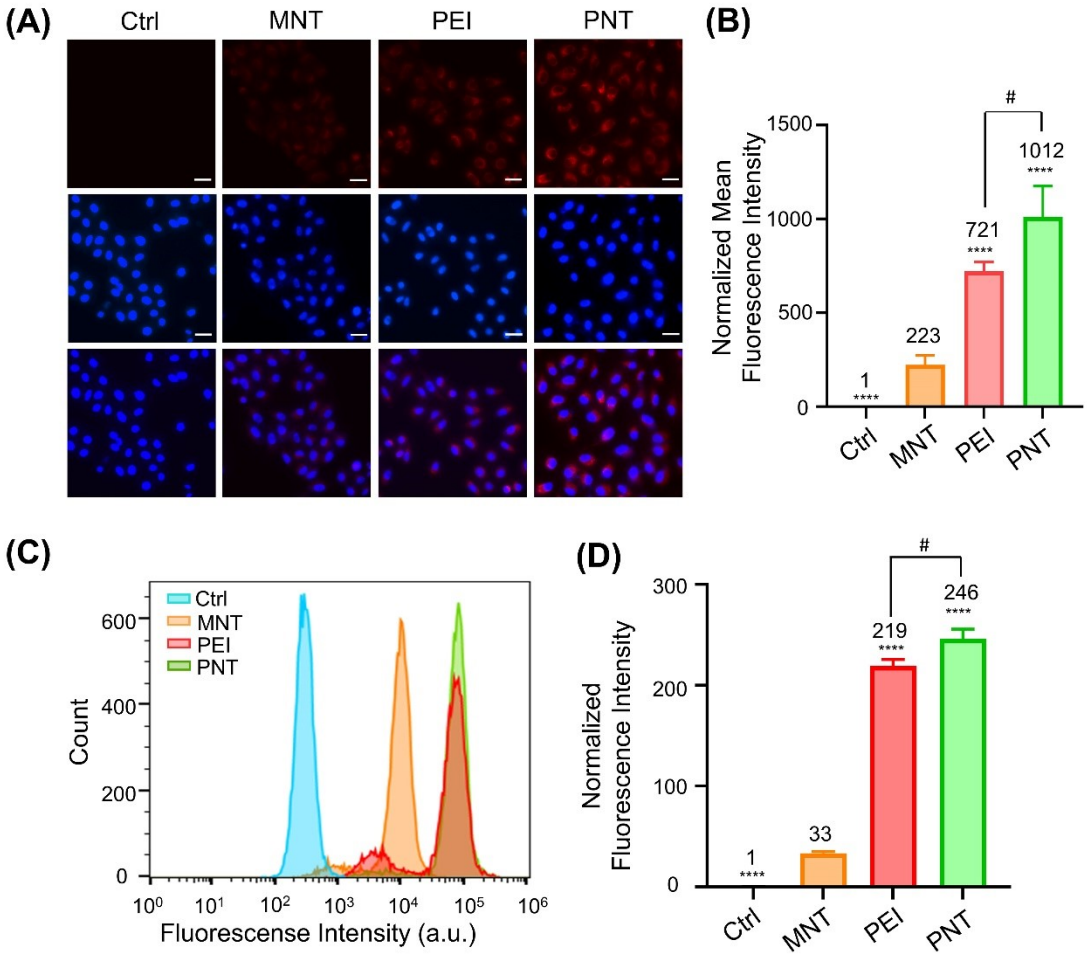

Fig. S3 Comparison of cellular uptake of PNT and PEI on A549 cell line. (A) Fluorescence images of PNT, MNT and PEI after a 24-h incubation with A549 cells. Each group contained a Cy3 concentration of 300 nM, and cell nuclei were stained with Hoechst 33342. The scale bar is 20 μm. (B) Semi-quantification of the fluorescence intensity in (A). (C) Flow cytometry analysis was conducted to assess the cellular internalization of the three groups mentioned in (A), with cell incubated in pure medium serving as the control. (D) Mean fluorescence analysis of the groups in (C). All data present as mean value ±SD (n=5). One-Way ANOVA was used for statistical analysis. ** $P < 0.01$, **** $P < 0.0001$, compared to the MNT group. # $P < 0.05$, comparison between the two connected groups.

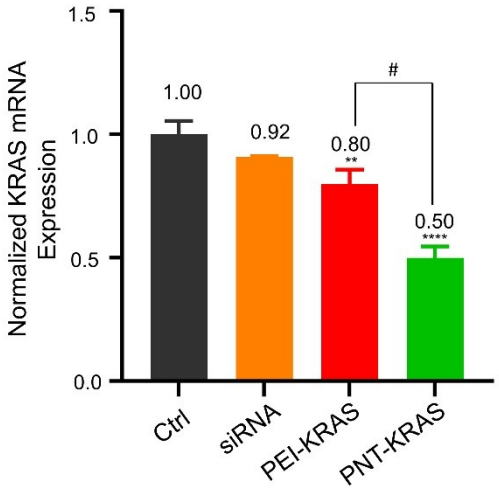

Fig. S4 A comparison of gene silencing effects of PNT and PEI for KRAS siRNA. RT-qPCR was performed to detect intracellular KRAS mRNA expression after treatment. All data present as mean value ±SD (n=5). One-Way ANOVA was used for statistical analysis. ** $P<0.01$, **** $P<0.0001$, compared to the control group. # $P<0.05$, comparison between the two connected groups.